Peng Hong-bing*, Chen Wei-qing, Chen Lie and Guo Dong

Effect of Tin on Hot Ductility and High-temperature Oxidation Behavior of 20CrMnTi Steel

Abstract: The hot ductility and high-temperature oxidation behavior of 20CrMnTi steel with 0.02% Cu and *x*% Sn ($0.004 \leqslant x \leqslant 0.049$) were investigated. The results show that tin has no significant effect on tensile strength of sample with less than 0.049% Sn. The critical temperature where the hot ductility reduces dramatically rises with the increase of tin content while the hot ductility decreases with its increase. The average tin content at austenite grain boundaries (GB) and substrate is 0.108% and 0.045% respectively in the specimen containing 0.049% tin quenched after heated to 1223 K and held for 600 s. Sn-segregation at the GB deteriorates the hot ductility. There is no direct relationship between the cause of the ductility trough and tin. However, Sn-segregation at the GB causes it to deepen a lot. The tin content should be controlled below 0.021%, which would not deteriorate the hot ductility significantly. There is no tin-enrichment at the scale/substrate interface when tin content is less than 0.049%. Moreover, although Sn is enriched under the steel surface, any liquid Sn-enrichment wasn't observed at the oxide/steel interface even in as high as 0.45% Sn-bearing steel with 0.02% Cu.

Keywords: tin, 20CrMnTi steel, hot ductility, high-temperature oxidation behavior

PACS® (2010). 81.40.-z

***Corresponding author: Peng Hong-bing:** State Key Laboratory of Advanced Metallurgy, University of Science and Technology Beijing, Beijing 100083, China. E-mail: phbing1021@126.com
Chen Wei-qing: State Key Laboratory of Advanced Metallurgy, University of Science and Technology Beijing, Beijing 100083, China
Chen Lie, Guo Dong: Xining Special Steel Co. Ltd., Xining 810005, China

1 Introduction

Although the route of scrap-based electric arc furnaces (EAFs) saves energy, raw material and cost compared with the conventional blast furnace/basic oxygen furnace (BF/BOF) route, the negative influence of residual elements such as surface hot shortness and deteriorating hot ductility limits steel manufacturing via EAF-based techniques. Cu, Sn, As and Sb are the common residual elements in steel scrap. When high-Cu residual containing steel undergoes oxidation during steelmaking processes, Fe will preferentially oxidize, and as a result, Cu enriches at the oxide/steel interface because it is nobler than Fe. At temperature above 1373 K, which is usually encountered in the secondary cooling, reheating and hot rolling processes, a Cu-rich liquid layer forms once the enrichment of Cu exceeds its solubility in the γ-Fe. The Cu-rich liquid could penetrate into γ-Fe grain boundaries and cause intergranular decohesion. Consequently, the steel surface will crack when mechanical load is applied, for example, in the rolling process because of the weakened grain boundaries by the liquid phase [1, 2].

Sn, Sb and As can decrease Cu solubility in γ-Fe phase and the melting point of Cu-rich phase to various extents and cause the hot-shortness tendency increase [3, 4]. The influences of these residual elements on Cu solubility in the solid γ-Fe phase at 1473 K were summarized by Melford [5], which showed that As only slightly decreases Cu solubility, but Sn and Sb decreases the solubility greatly. In prior work, it has also been reported that Sn at content as low as 0.03% promotes significant Cu-rich liquid grain boundary penetration and cracking in Fe-0.3%Cu-*x*%Sn ($0.03 \leqslant x \leqslant 0.15$) alloys after short time oxidation in air at 1423 K [6]. Moreover, Sn [7] could segregate in the Fe grain boundaries at moderate temperature range (673 K to 873 K). Therefore, a decrease in impact toughness often occurs in residuals containing steel when heated in or cooled slowly through this temperature range, which is known as temper embrittlement. Based on the pair bonding energy of elements present at the Fe grain boundary, Seah [8] predicted that Sn and Sb will be highly embrittling, whereas As and Cu has reduced effects.

Additionally, the tin content is large in the products such as 20CrMnTi steel of Xining Special Steel. Therefore this article focuses on the effect of the tin on the hot ductility and high-temperature oxidation behavior of 20CrMnTi steel with a low level of Cu content (0.02%). Moreover, the critical content of tin in 20CrMnTi steel has also been discussed in detail.

Table 1: Chemical composition of test steels (mass fraction, %)

Samples	C	Si	Mn	P	S	Cr	Ti	Cu	Sn	O	N
A	0.18	0.28	1.08	0.020	0.010	1.11	0.10	0.02	0.004	7 ppm	22 ppm
B	0.19	0.27	0.85	0.018	0.005	1.13	0.07	0.02	0.021	11 ppm	26 ppm
C	0.19	0.26	1.08	0.020	0.005	1.08	0.09	0.02	0.049	7 ppm	27 ppm
D	0.21	0.24	1.08	0.018	0.002	1.06	0.09	0.02	0.45	–	–

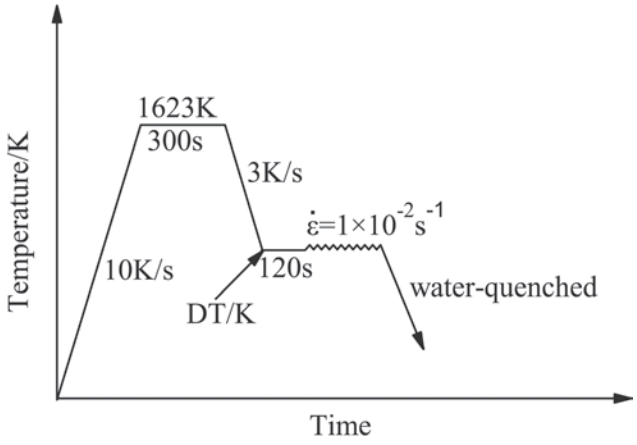

Fig. 1: Thermal schedule of the hot tensile test

2 Experimental

Table 1 shows the chemical composition of the samples. These samples (A, B, C and D) were prepared in vaccum induction furnace. After forged, sample A, B and C were machined into the thermal simulation tensile samples with dimension of Φ10 × 120 mm and the rest of A, B, C and sample D were machined into the high-temperature oxidation samples with dimension of 10 mm × 10 mm × 10 mm.

Fig. 1 shows the thermal schedule of the hot tensile test. This test was investigated by Gleeble-1500 thermal simulation machine. In this test, the specimens were heated up with the heating rate of 10 K/s to 1623 K under Ar atmosphere, held at this temperature for 300 s, and then cooled to the deformation temperature (DT), which are 973, 1023, 1073, 1123, 1173, 1223, 1273, 1323, 1423 and 1523 K, with the cooling rate of 3 K/s. After holding at DT for 120 s, the tensile test was performed with the strain rate of 1×10^{-2} s^{-1}. After fractured and then injection water cooling in 0.5 s, these specimens were water-quenched to the room temperature in order to keep the microstructure near the fracture at DT. The reduction in area (RA) of the specimens was used as a characteristic value for the hot ductility of the tested steel.

Moreover, in oxidation experiment, the samples were oxidized in an air atmosphere at various temperatures between 1273 K and 1473 K for 1800 s and 3600 s, and cooled in air to room temperature. The temperature was measured with a B-type thermocouple placed just beneath the specimen and controlled with in ±5 K of the set temperature. The fracture morphology of tensile specimens and the microstructure and composition of the oxide/steel interface were analyzed by using scanning electron microscope (SEM) equipped with energy diffraction spectrum (EDS).

The Sn content on substrate and grain boundaries was investigated in a JEOL JXA-8100 Electron Probe Microanalyzer (EPMA) equipped with wavelength dispersive X-ray spectrometer (WDS). The analysis was conducted on the substrate by 10 random points and grain boundary by 10 random points with accelerating voltage of 20 KV and a beam size of 1.0 μm.

3 Results

3.1 Hot ductility

Fig. 2 shows the relationship between the temperature and the tensile strength under different tin contents. Obviously, the tensile strength reduces as the temperature increases. And tin has no significant effect on high-temperature tensile strength because each sample has the similar tensile strength under different temperatures.

Fig. 3 shows the reduction in area for each sample. In the region from 973 K to 1323 K, $RA^A > RA^B > RA^C$ at the same temperature and there is a little tiny difference between RA^A and RA^B, and especially in 1223 K~1073 K, the RA reduces obviously with the increase of the tin content. The RA for sample A, B, and C is defined as RA^A, RA^B and RA^C respectively. The temperatures, at which deteriorated the hot ductility dramatically, were different; the sample B and C were both at 1273 K while the sample A was at 1223 K. It can be concluded that with the increase of the tin content, the critical temperature, where the hot ductility

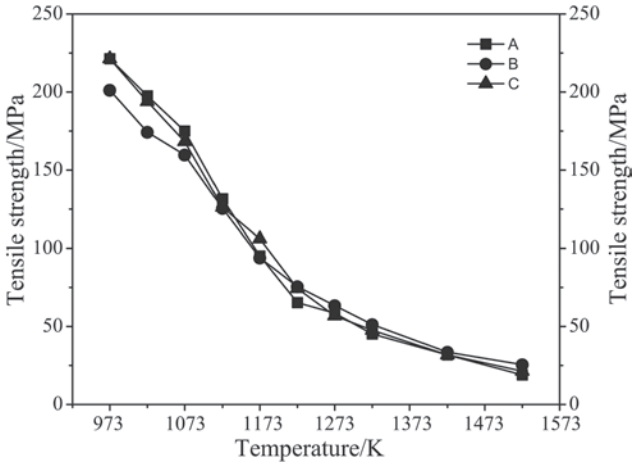

Fig. 2: Relationship between the tensile strength and the temperature

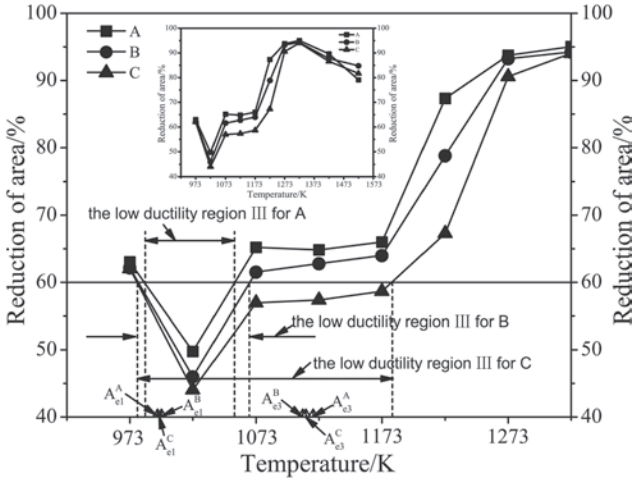

Fig. 3: Relationship between the reduction of area and the temperature

reduces dramatically, gets much higher. And at the same temperature, the hot ductility gets much worse with the increase of the tin content. Considering the RA of 60% [9, 10], under which was considered as the low ductility. So, the low ductility region III for sample A, B and C are 985.22~1055.67 K, 978.78~1067.78 K and 978.78~1181.89 K, respectively. And they were labeled on Fig. 3. It can be inferred that the range of low ductility region III became large with the increase of the tin content. In the low ductility region III, the percentage reduction of area for each sample first drops and then rises, and there exists a ductility trough for each sample at 1023 K. However, the ductility troughs of sample B and C containing high tin are deeper than that of sample A.

According to the empirical formulae for the calculation of transformation temperatures [11], the calculation value of A_{e1}^{A}, A_{e3}^{A}, A_{e1}^{B}, A_{e3}^{B}, A_{e1}^{C}, A_{e3}^{C} were 995.055 K, 1118.434 K, 998.145 K, 1110.049 K, 995.13 K, 1112.652 K, respectively. The A_{e1}^{x} and A_{e3}^{x} were defined as the A_{e1} and A_{e3} temperatures of sample x (x = A, B, C) here and they were also illustrated in the Fig. 3.

3.2 Fracture morphology and EPMA analysis

Fig. 4 shows the fracture morphology of three samples at 1223 K. It can be drawn that the micro-feature of sample A and B is ductile fracture, on which has a large quantity of huge and deep dimples; while the fracture morphology of sample C presents the “rock candy shape”, which is the typical intergranular fracture. It can be concluded that the brittle fracture is caused when the hot ductility is reduced greatly, which happens in the specimen containing more than 0.049% tin. However, the hot ductility is less affected in 20CrMnTi steel containing less than 0.021% tin.

Two metallographic specimens were machined from the sample C and then water-quenched after holding at 1223 K for 600 s and both of them did not undergo the tensile test. One was eroded with picric acrid for spot scan random at the GB by EPMA and the other was not eroded for spot scan random on the substrate. The result can be

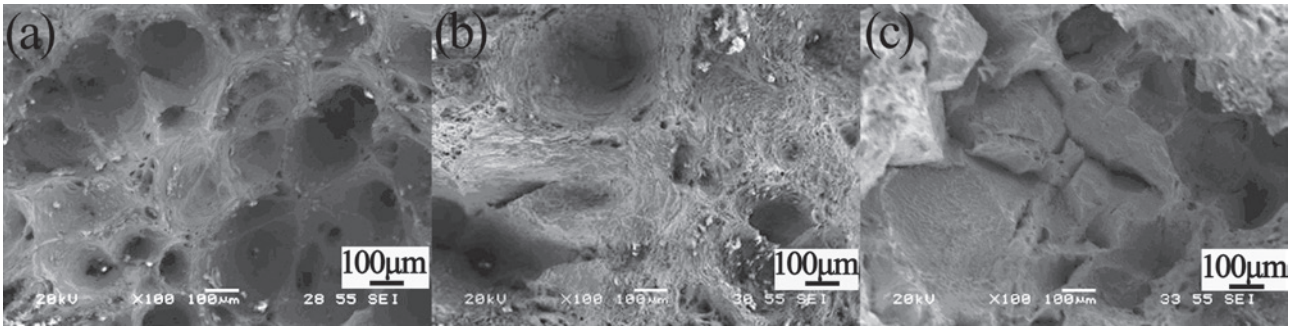

Fig. 4: Fracture morphology of samples at 1223 K: (a) sample A; (b) sample B; (c) sample C

Table 2: Results of qualitative analysis of sample C tested by EPMA (mass fraction, %)

Points	1	2	3	4	5	6	7	8	9	10	Avg.	SD	SEA
Substrate	0.069	0.045	0.055	0.061	0.054	0.038	0.027	0.040	0.023	0.037	0.045	0.0148	0.00467
GB	0.095	0.102	0.108	0.086	0.131	0.098	0.119	0.136	0.070	0.136	0.108	0.0222	0.00703

Note: Standard deviation, $SD = \sqrt{Var}$, where $Var = \frac{1}{n-1}\sum_{i=1}^{n}(C_{Sn,i} - C_{Sn,avg.})^2$. Standard error of the average, $SEA = \frac{SD}{\sqrt{n}}$; and $n = 10$.

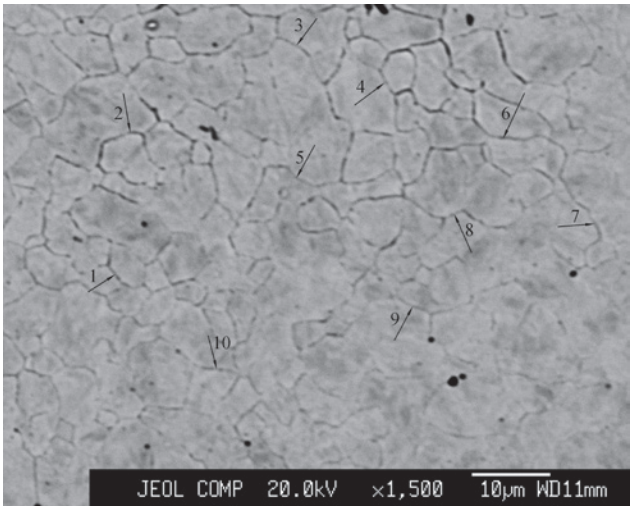

Fig. 5: Spot scan by EPMA at the grain boundary of sample C

shown in Table 2 and Fig. 5. The average tin content on the substrate and the grain boundary is 0.045% and 0.108% respectively. It shows there is an obvious tin segregation at the austenite grain boundary in sample C. Considering the $RA^A > RA^C$ at the same temperature and the sample A which was the comparative sample produced without adding Sn. It can be inferred that Sn-segregation at the austenite grain boundary decreases the RA^C and therefore deteriorates its hot ductility.

3.3 Micro-morphology of oxide layer

The tin-enrichment was not observed at the oxide/substrate interface investigated in SEM on the condition of the sample with less than 0.049% tin oxidized between 1273 K and 1473 K for 1800 s and 3600 s. For the same oxidizing time, the thickness of oxide layer increases as the temperature rises. When the sample B was oxidized for 1800 s at 1273 K, 1373 K and 1473 K, its thickness of oxide layer was 186.70 μm, 293.35 μm, and 409.93 μm respectively. When the sample C containing 0.049% tin was oxidized for 3600 s at 1373 K, its micro-morphology could be seen in Fig. 6(a). There was an obvious stratification in the oxide layer. EDS shows that the outer oxide is Fe_xO_y. The oxide layer near the interface also contains some other elements such as Cr, Si (listed in Table 3). However, any Sn-enrichment was not observed at the oxide/substrate interface.

Table 3: Chemical composition of outer oxide and the oxide nearby the substrate (mass fraction, %)

Elements	Fe	Cr	Si	O
The outer oxide	79.23	–	–	20.77
The oxide nearby the substrate	74.58	5.26	3.37	16.8

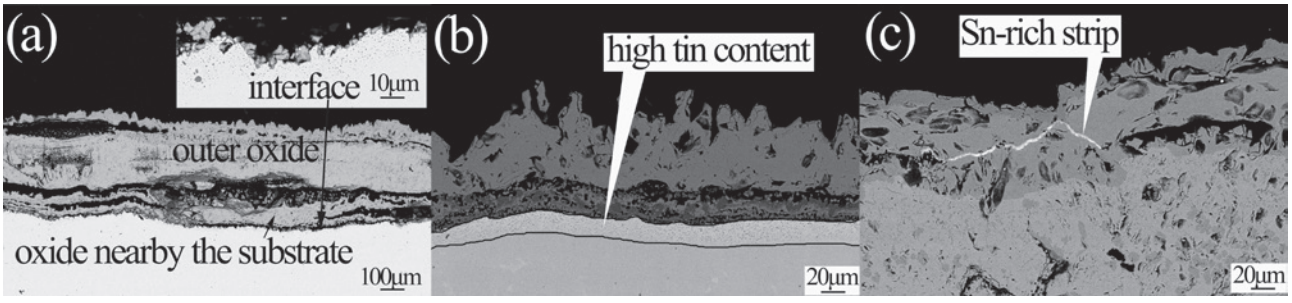

Fig. 6: Morphology of the oxide/substrate interface at 1373 K: (a) sample C oxidized for 3600 s; (b) the oxide/substrate interface of sample D oxidized for 1800 s; (c) the oxide layer of sample D oxidized for 1800 s

In order to further investigate whether liquid Sn-enrichment can form at the oxide/steel interface in the steel with 0.02% Cu and high Sn content. The sample D with 0.02% Cu and 0.45% tin was produced. Fig. 6(b) and (c) were the micro-morphologies of the oxide layer when the sample D was oxidized at 1373 K for 1800 s. There is a weak white belt at the substrate surface (marked in the black line in Fig. 6(b)). EDS shows the tin content is over 4.11% in this area. It is concluded from the quantitative analyses that Sn diffuse back into the steel and is not enriched at the oxide/steel interface. In Fig. 6(c), there is a white line in the oxide layer. Its chemical composition is mainly Fe, O and Sn and the tin content is above 35.09%.

4 Results discussion and analysis

4.1 Effect of tin on the hot ductility

There is a significant difference between the fracture morphology of sample C and sample A and B at 1223 K. The morphology of sample C is the intergranular brittle fracture. It can be found that tin has an obvious segregation at the austenite grain boundary in the quenching sample C. Considering the $RA^A > RA^C$ at the same temperature and the sample A which was the comparative sample produced without adding Sn, it is inferred that Sn-segregation at the GB deteriorates the hot ductility of 20CrMnTi steel. The grain boundary segregation of tin reduces the surface energy of the grain boundary, weakens the intergranular cohesion, accelerates the nucleation and growth of the grain boundary voids and impedes the grain boundary migration and dynamic recrystallization [12, 13] and thus it worsens the hot ductility of 20CrMnTi steel.

In prior work [13–15], two main mechanisms could explain the ductility trough. The first mechanism is mainly associated with the carbides and/or nitrides of some elements such as Nb, V, Ti precipitating at the grain boundary in the single-phase region (austenite) and then voids occurred and then deteriorated the hot ductility. The other is that the proeutectoid ferrite film precipitates along the austenite grain boundaries in the two-phase region (ferrite and austenite). The ferrite yield strength is relatively low compared with that of the austenite. It is easy to form stress concentration on the ferrite film and then reduces the hot ductility. The three samples all exist TiN at the austenite grain boundary by SEM, illustrated in Fig. 7. The precipitation temperature of TiN in sample A, B and C was 1743 K, 1728 K and 1751 K respectively. They were worked out by $\log([Ti]\cdot[N])_\gamma = 5.4 - 15790/T$ [16]. However, the temperature of the ductility trough is 1023 K. At this temperature, all steels are in the two-phase region instead of the austenitic single-phase region. So it can be concluded that TiN at the austenite grain boundary was not the main reason to cause the ductility trough. Fig. 8 shows the metallographic structure nearby the fracture at 1023 K of the three samples. Obviously, the proeutectoid ferrite film precipitates along the austenite grain boundary in each sample. Therefore, the main reason causing the ductility trough at 1023 K was the precipitation of proeutectoid ferrite film along the austenite grain boundary.

The three samples have a similar shape of the hot ductility curve in the low ductility region III. The ductility troughs all appear at 1023 K, which becomes much deeper with the increase of tin content. So there is no direct relationship between the cause of the ductility trough and tin. However, the precipitation of proeutectoid ferrite film

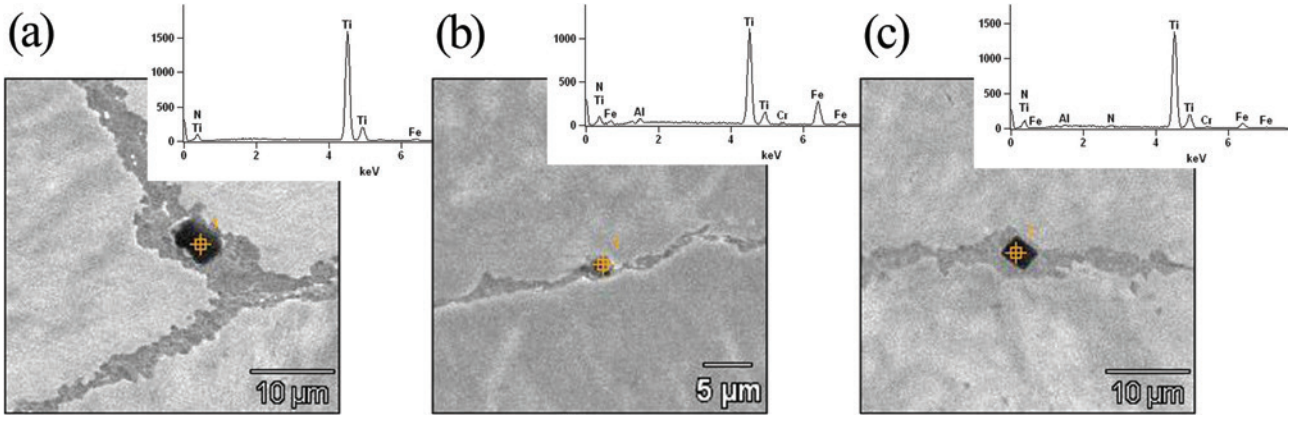

Fig. 7: Precipitates at the austenite grain boundary: (a) sample A; (b) sample B; (c) sample C

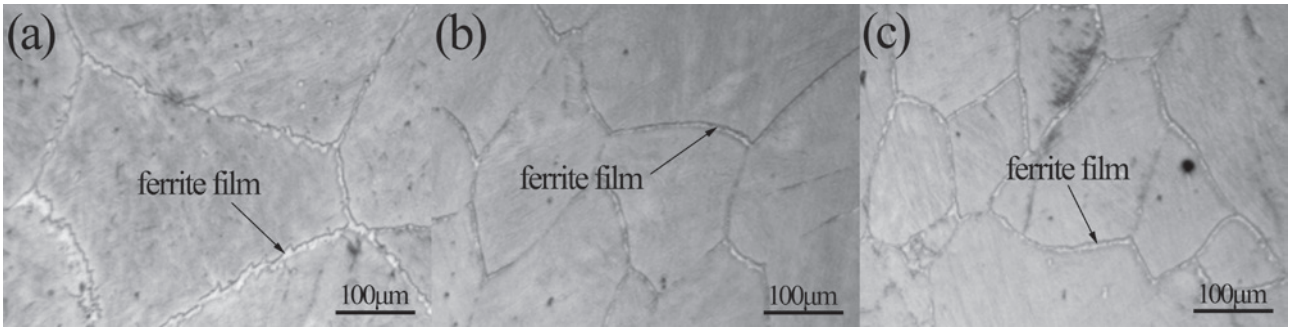

Fig. 8: Metallographic structure nearby the fracture at 1023 K: (a) sample A; (b) sample B; (c) sample C

along the austenite grain boundary combined with tin segregation at the GB can cause the ductility trough to become deeper.

4.2 Effect of tin on high-temperature oxidation behavior of 20CrMnTi steel

When residual elements such as Cu, Sn and As containing steel undergoes oxidation during steelmaking processes, iron will preferentially oxidize, and as a result, residual elements enrich at the oxide/steel interface because it is nobler than Fe. Once the enrichment of residual elements exceeds its solubility in the γ-Fe phase and penetrates into γ-Fe grain boundaries and causes intergranular decohesion, the surface will crack when mechanical load is applied, which will deteriorate the surface quality of steel products.

Fe-0.3%Cu-*x*%Sn ($0.03 \leqslant x \leqslant 0.15$) alloys have been investigated for high temperature oxidation behavior by Yin [1, 6], and liquid phase was found to enrich at the oxide/steel interface and Sn promotes significant hot cracks at level of 0.03%. So, it is essential to study alloys with very low Cu content and various Sn contents for this behavior. Therefore, the sample containing 0.02%Cu-*x*%Sn ($0.004 \leqslant x \leqslant 0.45$) has been investigated in this article. It can be found that, when the Sn content was less than 0.049%, there was no tin enrichment at the oxide/steel interface and this might suggest that the cracking would not take place because liquid Sn-enrichment was not formed at the oxide/steel interface. In order to further investigate whether there is Sn-enrichment at the oxide/steel interface in the specimen with high Sn content, the sample D (listed in Table 1) was made for the high-temperature oxidation experiment. Fig. 6(b) shows the BSE image at the oxide/steel interface of sample D. Although the Sn concentration under the steel surface was analyzed by EDS to be more than 4.11%, any Sn-enrichment was not observed even in as high as 0.45% Sn bearing steel with 0.02% Cu. It is speculated from the quantitative analyses that Sn diffuses back into the steel during oxidation and is not enriched at the oxide/steel interface.

Moreover, the diffusion coefficient of Sn in γ-Fe is large, which is 1.9×10^{-14} at 1373 K [17], and there is plenty of time for diffusion during the heating of the sample, tin will dissolve in the steel substrate by its diffusion instead of segregating at the oxide/steel interface. In addition, for Fe-Sn binary system, the solubility limit of Sn in α-Fe is large as about 16% at 1373 K and the diffusion coefficient of Sn in α-Fe is also large about 7.9×10^{-13} [17]. Thus even if Sn is enriched under the steel surface and the Sn-enriched regions change into α phase, liquid Sn-enrichment was not form at the oxide/steel interface in the steel with 0.02% Cu. From this, it might be inferred that no liquid Sn-enrichment was formed and would not cause surface cracks in Sn-bearing steel with 0.02% Cu.

5 Conclusions

1. Tin has no great effect on the tensile strength of sample with less than 0.049% Sn. The low ductility region III for sample A, B and C are 985.22~1055.67 K, 978.78~1067.78 K and 978.78~1181.89 K, respectively. The critical temperature where the hot ductility reduces dramatically rises with the increase of tin content, while the hot ductility decreases with its increase. The critical tin content, under which the hot ductility of specimen is not deteriorated significantly, of 20CrMnTi steel with 0.02% Cu is 0.021%.
2. In the region from 973 K to 1323 K, $RA^A > RA^B > RA^C$ at the same temperature and there is a little tiny difference between RA^A and RA^B. The average tin content of the austenite grain boundary and the substrate is 0.108% and 0.045% respectively in sample C contain-

ing 0.049% Sn. Considering the $RA^A > RA^C$ at the same temperature and the sample A which is produced as the comparative sample without adding Sn. It can be inferred that Sn-segregation at the austenite grain boundary decreases the RA^C and therefore deteriorates its hot ductility.

3. There is no direct relationship between the cause of the ductility trough and tin. It is the precipitation of proeutectoid ferrite film along the austenite grain boundary that causes the ductility trough at 1023 K in sample A, B and C. Moreover, the precipitation of proeutectoid ferrite film along the austenite grain boundary combined with tin segregation at the GB cause the ductility trough to deepen a lot in sample C.
4. The oxide layer becomes thicker with the increase of the oxidizing temperature. And Sn-enrichment is not observed at the oxide/steel interface in the sample containing less than 0.049% Sn. Moreover, although the Sn content under the steel surface is more than 4.11%, any Sn-enrichment is not observed at the oxide/steel interface even in as high as 0.45% Sn-bearing steel.

Received: March 13, 2013. Accepted: July 27, 2013.

References

[1] Yin L, Sridhar S. Effects of Residual Elements Arsenic, Antimony, and Tin on Surface Hot Shortness. Metallurgical and Materials Transactions B. 2011, 42(5): 1031–1043.
[2] Garza L G, Van Tyne C J. Surface Hot-shortness of 1045 Forging Steel with Residual Copper. Journal of Materials Processing Technology. 2005, 159(2): 169–180.
[3] Okamoto H. Desk Handbook: Phase Diagrams for Binary Alloys. ASM International, Materials Park, OH, 2000.
[4] Salter J M J. Effects of alloying elements on solubility and surface energy of copper in mild steel. Journal of the Iron and Steel Institute. 1966, 204(5): 478–488.
[5] Melford D A. The Influence of Residual and Trace Elements on Hot Shortness and High Temperature Embrittlement. Philosophical Transactions of the Royal Society of London A. 1980, 295(1413): 89–103.
[6] Yin L, Sridhar S. Effects of small additions of tin on high-temperature oxidation of Fe-Cu-Sn alloys for surface hot shortness. Metallurgical and Materials Transactions B. 2010, 41(5): 1095–1107.
[7] Seah M P, Hondros E D. Grain boundary segregation. Proceedings of the Royal Society of London A. 1973, 335(1601): 191–212.
[8] Seah M P. Adsorption-induced interface decohesion. Acta Metallurgica. 1980, 28(7): 955–962.
[9] Suzuki H G, Nishimura S, Imamura J. Embrittlement of steels occurring in the temperature range from 1000 to 600 °C. Transactions of the Iron and Steel Institute of Japan. 1984, 24(3): 169–177.
[10] Suzuki H G, Nishimura S, Imamura J, et al. Hot ductility in steels in the temperature range between 900 and 600 °C. Tetsu-to-Hagane. 1981, 67(8): 1180–1189.
[11] Andrews K W. Empirical formulae for the calculation of some transformation temperature. Journal of the Iron and Steel Institute. 1965, 203(7): 721–727.
[12] Nagasaki C, Kihara J. Effect of Copper and Tin on Hot Ductility of Ultra-low and 0.2% Carbon Steels. ISIJ International. 1997, 37(5): 523–530.
[13] Nachtrab W T, Chou Y T. High Temperature Ductility Loss in Carbon-manganese and Niobium-treated Steels. Metallurgical and Materials Transactions A. 1986, 17(11): 1995–2006.
[14] Ouchi C, Matsumoto K. Hot Ductility in Nb-bearing High-strength Low-alloy. Transactions of the Iron and Steel Institute of Japan. 1982, 22(3): 181–189.
[15] Nachtrab W T, Chou Y T. The Effect of Sn, Al, and N on the Hot Ductility of a Carbon-manganese Steel between 700° and 1200 °C. Metallurgical and Materials Transactions A. 1988, 19(5): 1305–1309.
[16] Yan-Zhi L, De-Lu L, Xin-Ping M, et al. Titanium Carbonitrides in Ti-Microalloyed Steels Produced by CSP Process. Iron & Steel. 2010, 45(2): 70–73.
[17] Imai N, Komatsubara N, Kunishige K. Effect of Cu, Sn and Ni on Hot Workability of Hot-rolled Mild Steel. ISIJ International. 1997, 37(3): 217–223.